The Pharmaceutical and Chemical Journal, 2018, 5(2):144-166

Available online www.tpcj.org

Research Article

ISSN: 2349-7092
CODEN(USA): PCJHBA

Diffusion Influenced Non-equilibrium Gating Processes of a Voltage-gated Potassium Ion Channel

Biswajit Das, Gangopadhyay

S.N. Bose National Centre for Basic Sciences, Block-JD, Sector-III, Salt Lake, Kolkata-700098, India.

Abstract Here we have studied the kinetics as well as the energetics of a diffusion influenced nonequilibrium gating process of a voltage-gated K-channel for a oscillatory voltage through the master equation description. A diffusion-influenced five-state Hodgkin-Huxley type voltage-gated scheme is proposed on the basis of the established findings that the K-ions can diffuse through a mutated voltage sensing domain even if the channel protein remains in the closed conformation. At moderate frequencies of the oscillatory voltage, the dynamic hysteresis behaviour shown by the kinetic and thermodynamic response properties of this channel protein are annihilated by the diffusion of K-ions at diffusion controlled limit. Moreover, for oscillating voltage the diffusion time scale interferes with the intrinsic time scale of the ion-channel producing a beating phenomenon in the current signal whose modulation depth depends on the diffusion rate. At reaction-controlled limit, the time periodic oscillation of the total entropy production rate shows the symmetric behaviour over the two half cycles at extreme high frequencies, but at diffusion-controlled limit such symmetry is destroyed.

Keywords Voltage gated K channel; mutated voltage sensing domain; diffusion influenced gating; nonequilibrium thermodynamics; dynamical hysteresis

Introduction

Study of the kinetics as well as the energetics of a single voltage-gated potassium ion channel(VGKC) is gaining increasing attention in neurobiology as it plays an important role in the generation and propagation of the action potential, the nerve impulse, in the living excitable cells e.g., neurons or muscle cells [1, 2, 3, 4, 5]. A VGKC is a trans-membrane electrical sensitive tetrameric protein, where each monomer is composed of six transmembrane segments (TS), designated as S1-S6, which form two structurally and functionally different parts [6, 7, 8, 9, 10, 11, 12]. The first four TS (S1-S4) form the voltage-sensing domain (VSD), positioned at the periphery of the channel within the lipid membrane and the others two, S5-S6 make the pore-forming domain (PFD), which are located in the channel centre [7, 8, 9]. The VSD and PFD are structurally coupled by the S4-S5 linker [7, 8, 9]. The PFD includes a channel gate (CG) along with a selectivity filter (SF), which make the ion conducting pathway with a central ion conducting pore (CICP) through which the K-ions diffuse from inside to outside of the cell membrane down through an electro-chemical gradient near diffusion limited rates (10^7 ions channel^{-1} sec^{-1}) [8, 9]. At equilibrium resting membrane potential, the four PFDs of four monomers remain in such a conformation which does not allow the diffusion of K-ions through the CICP [7, 8, 9, 10, 11]. However, upon sensing the membrane potential difference in an independent way, the four VSDs of four monomers change their structural conformation, which accelerates in changing the conformation of the PFDs so that the K-ions can diffuse through the CICP [7, 8, 9, 10, 11].

In living cell, the working of a VGKC is initiated during depolarisation of the cell, which is basically a non-equilibrium phenomenon with respect to cell's resting equilibrium state [1, 2, 13]. To explore the non-equilibrium

working principle of a VGKC, recently, non-equilibrium response spectroscopy is being used extensively [14, 15, 16, 17]. In this technique, an externally modulated continuous voltage pulse is supplied to a VGKC so that the channel protein shows its far from equilibrium response [14, 15, 16, 17]. The motivations of these non-equilibrium studies lie in exploring the proper mechanism of voltage-gating of a single VGKC, along with the exploration of gating-dynamics from kinetic and energetic view point [13, 14, 15, 16, 17]. For pursuing the study on gating-dynamics, till now, several Markov models have been proposed.

However, at non-equilibrium environment, the most useful gating-model is the five-state Hodgkin-Huxley type gating-scheme (HHGS) [16], where five dynamical states of a VGKC are considered on the basis of the counting of the number of monomers remaining in the active or ion-conducting conformational state at any instant of time [13, 12, 18, 19]. In this gating scheme, it is assumed that each monomer of a VGKC has two conformations, active (ion-conducting) and inactive (non-conducting) conformational states. Each monomer works independently, and the conformational change of a monomer is a stochastic event [18, 13, 19]. The corresponding gating-dynamics are described through HHGS in terms of the one-dimensional random walk motion in the conformational state space of a VGKC, where the transition probabilities between two successive Markov states are considered as a function of voltage [18, 13, 16, 19]. In this circumstance a natural question arises: Why the transition probabilities in HHGS are only function of voltage? Does the other physiological factors, such as the diffusive motion of K-ions influence the transition probabilities in HHGS?

The influential possibility of the diffusion of K-ions on the gating-dynamics also comes in our mind after studying the recent work of Khalili-Araghi *et al.,* [11], where it is observed that the mutation of first gating arginine (R1) on the S4 segment to smaller uncharged amino acids such as serine or asparagine will turn the VSD into an ion channel, which allows the permeation of cations including K-ions through the helical bundle even if the CICP remains closed [11]. They have also reported that the diffusion of K-ions through the VSD produces the omega current, which is totally different from the K ionic-current [11].

In this aspect, our question is that if the gating dynamics is studied for the mutated VGKC, then does the diffusion of K-ions influence the transition probabilities of the gating mechanism? Secondly, if the diffusive motion of K-ions can influence the gating dynamics, then the other question is that how can we theoretically study the diffusion influenced gating process of a mutated VGKC through the HHGS at non-equilibrium? To search in this direction here we have proposed a diffusion influenced HHGS for a mutated VGKC and the corresponding method is developed to study the diffusion influenced gating-dynamics. In our theory, the transitions between two successive Markov states are not only function of voltage, rather they are function of the applied voltage along with the diffusion of K-ions. To understand the effect of the diffusion on the gating dynamics, here the kinetics as well as the non-equilibrium energetics have been studied in presence of the external oscillating voltage through the master equation approach. Our study reveals several diffusion influenced biophysical properties of the gating dynamics of a single VGKC at non-equilibrium environment.

The paper is organized as follows. In section 2, we have proposed a diffusion influenced five-state Hodgkin Huxley type gating-scheme. The corresponding model to describe the non-equilibrium diffusion influenced VGKC-dynamics as well as the corresponding energetics through the master equation description are discussed in section 3. In section 4, the numerical analysis are carried out to study the diffusion influenced kinetic and thermodynamic properties of a VGKC. Finally, the paper is concluded in section 5.

2. Diffusion influenced voltage-gating scheme of a VGKC

In this section, the five-state Hodgkin Huxley type voltage-gated scheme is discussed in terms of the functional activities of PFD and VSD for the non-mutated and mutated VGKC. The word 'mutated VGKC' signifies that the VSDs of a VGKC are mutated. Here we the non-mutated case is considered for understanding the necessity of the consideration of the mutated case to describe the diffusion influenced gating dynamics of a VGKC.

Now, before going into the detailed description of the gating-schemes for the non-mutated and mutated cases, here, at first, we have briefly discussed the structural and functional connectivity between the PFDs and VSDs for understanding their role in governing the gating process. For this purpose, in Fig.1, a cartoon is drawn where the

activity of two monomers of a VGKC are depicted from the lateral view point for these two cases, where each monomer is depicted in the combination of one VSD and one PFD. The structural and functional studies of VGKC reveal that a PFD and a VSD possess several conformations during the voltage-dependent activation of a VGKC, however, for simplicity, here it is considered that the PFD has two conformations, inactive or non-conducting state and active or conducting state, whereas for VSD, they are the non-voltage sensing and the voltage-sensing conformations.

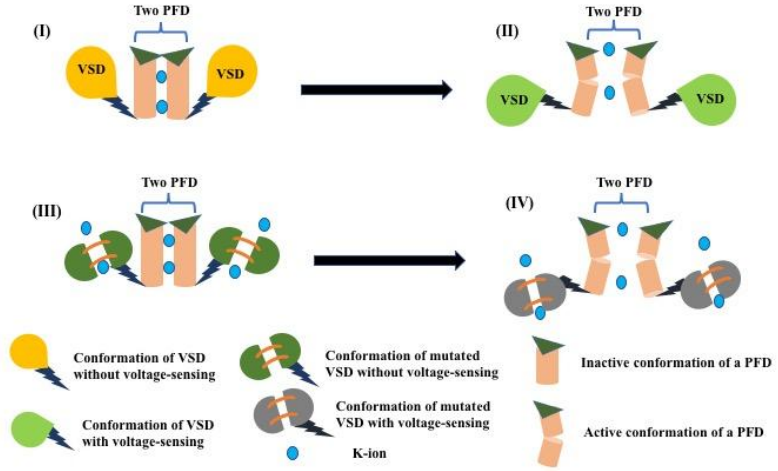

Figure 1: In figure (I) and (II), we have depicted the conformational changing of the PFDs from inactive to active conformational states for two monomers due to changing in the conformation of VSDs. Two figures are drawn for brief understanding about the activity of a normal or non-mutated VGKC where VSD's working only depends on the applied voltage. However, in (III) and (IV) we have described the same conformational changing phenomena for PFDs and VSDs when the VSDs are mutated. In this case, the K-ion permeation is possible through the VSDs when the PFDs remain inactive as well as in active state. In this case, the working of VSDs depend on the voltage and the diffusion of K-ions. For simplicity we consider only the diffusion of K-ions through the mutated VSDs. Here, we have considered that the conformation of VSDs for mutated and non-mutated cases are different, although the conformation remains the same for PFDs.

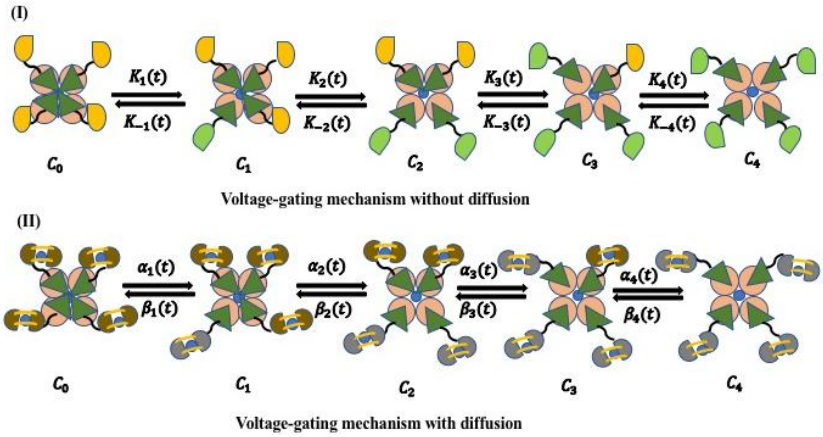

Figure 2: In (I), we have described the five state Hodgkin Huxley type voltage-gated scheme, where the transitions between two successive Markov states, $K_i(t)$ and $K_{-i}(t)$ with $i=1,...,4$ depend only on the voltage. However, in (II) the transitions between the two Markov states, $\alpha_i(t)$ and $\beta_i(t)$ with $i=1,...,4$ depend on the voltage as well as the diffusion of K-ions through the mutated VSD. In (I) and (II), the gating mechanism is operated due to

conformational change of VSDs, which is already described in the previous figure, Fig1. The colours used to designate the conformations for VSDs and PFDs in mutated and non-mutated cases are the same like in Fig1.

In Fig.1 (I) and (II), we have described the conformational changing of VSDs and PFDs when VSDs are non-mutated. In Fig.1(I) it is depicted that the two PFDs of two monomers remain in the inactive conformational state which hinders the diffusion of K-ions. However, upon sensing a voltage pulse, VSDs change their conformations from non-voltage sensing to voltage sensing conformation, which accelerates the conformational changing of PFDs from inactive to active state. Consequently, the K-ions can diffuse freely through the ion-conducting pathway, which is shown in Fig.1 (II). In these two figures, (Fig.1 (I) and (II)), no diffusive motion of K-ions is considered through the non-mutated VSDs, and that consideration is relevant with the functional activity of VSD at normal physiological condition[6, 7, 8, 9, 10, 11]. In this respect, we want to mention that for simplicity, in Fig.1 (II) we have shown that two PFDs goes to active conformation simultaneously for changing the conformations of two VSDs. Although, for constructing the gating scheme, here it is considered that at any instant of time two PFDs can't change their conformations simultaneously. But this consideration in Fig.1(II) does not affect in understanding the structural and functional connectivity between VSD and PFD in the gating process. Similar consideration is also taken in the case of mutated VGKC which is depicted in Fig.1 (III) and (IV). Moreover, the single molecule study of a VGKC infers that the conformational changing of a PFD and a VSD are a stochastic event and each monomer works in an independent way[12]. On the basis of this fact, in Fig.2(I), the five-state Hodgkin Huxley type Markov scheme is constructed for the non-mutated case, where the dynamical states are designated as C_n with $n = 1,..,4$ which represent the number of PFDs are in the active or conducting state at any instant of time. Here the activity of four PFDs and four VSDs are shown from the top view point, and the colour of the conformations of VSDs and PFDs remain same as in Fig.1 (I) and (II). In this scheme we can observe that due to changing the conformation of a VSD of a monomer, the conformation of the related PFD is changed, which results the transition from one Markov state to its adjacent states. Hence the transitions between the Markov states are governed mainly by the activity of the VSDs, and as in the normal physiological condition, the working of a VSD depends only on the voltage, so the transition probabilities $K_{\pm n}(t)$ in the gating scheme in Fig.2(I) should be the function of the voltage value, $V(t)$ at time t. For notational simplicity, here $K_{\pm n}(V(t))$ are represented as $K_{\pm n}(t)$, where $K_n(t)$ represents the forward transition probabilities, whereas the backward transition probability is designated as $K_{-n}(t)$ with $n = 1,...,4$.

From the discussion related to the gating scheme for the non-mutated case, we can infer that the influential possibility of the K-ionic diffusion on the gating dynamics may arise if the K-ions can permeate through the VSDs. Recent study of Khalili-Araghi *et al.* [11] infers that the mutation in the amino acid sequence in VSDs allows the permeation of K-ions through the VSD. Based on this findings, here we have proposed a diffusion influenced gating-scheme, where we have assumed that upon sensing the voltage difference, a mutated VSD can also change its conformation, which accelerates the conformational changing of the PFD from inactive to active state as like in the non-mutated case. In Fig.1 (III), the mutated VSD is in the non-voltage-sensing conformation, whereas, Fig.1 (IV), represents the voltage-sensing conformation of a VSD. As mutation is carried out only in the VSDs, so in Fig.1 (III) and (IV), the conformations of a VSD are represented in different colours for mutated and non-mutated cases, whereas, in both cases, the conformations of a PFD remain same. The five-state gating scheme for the mutated VGKC is constructed by taking the similar consideration, as it is taken for the non-mutated case, and the diffusion-influenced gating scheme is shown in Fig.2 (II). The main difference between these two gating schemes is that in the mutated case, the transition probabilities between two Markov states are the function of both voltage as well as the diffusive motion of K-ions, whereas for non-mutated case, the transition probabilities are only dependent on the voltage. Hence in the mutated case, the forward and backward transition probabilities are designated as $\alpha_n(t)$ and $\beta_n(t)$, respectively where n runs from 0 to 4. Moreover, in the mutated gating scheme, K-ions can diffuse

through the CICP as well as the VSDs at C_4 Markov state, whereas, in non-mutated case, diffusion of K-ions occurs only through CICP when the channel protein remains in that Markov state.

3. Diffusion influenced Kinetics

Here we have described the diffusion influenced dynamics as well as the energetics of a single voltage-gated potassium ion channel through the master equation description for constant as well as for oscillating voltage. For constant voltage case, the connection between the master equation with the familiar Hodgkin-Huxley equation is discussed. The time-dependent solution of the ion-conducting state probability is then given for the low and high frequency values of the oscillating voltage which is derived from the master equation for the diffusion influenced VGKC-gating dynamics. Then the non-equilibrium energetics is described in terms of the system, medium and total entropy production rates. Finally, an energetic analysis is carried out to study whether the diffusion influenced VGKC dynamics is entropy or free-energy driven.

3.1. Master equation without Diffusion

For completeness of our study, here, at first, we have described the master equation for the voltage dependent gating-process of a single non-mutated VGKC, described in Fig.2 (I). For this five state Markov model, the master equation can be written as

$$\frac{dP_n(t)}{dt} = \sum_{\mu=\pm1}[w_\mu(n-\nu_\mu \mid n)(t)P_{(n-\nu_\mu)}(t) - w_{-\mu}(n \mid n-\nu_\mu)(t)P_n(t)], \tag{1}$$

where ν_μ is the stoichiometric coefficient of the μ-th reaction and $\nu_1 = 1$ for forward process and $\nu_{-1} = -1$ for backward process. $P_n(t)$ is the probability of having n number of subunits in active state at time t where n runs from 0 to n_T. Here n_T is the total number of subunits with $n_T = 4$. Here the forward transition probability, $w_1(n-1 \mid n)(t) = K_n(t)$ and the backward transition probability, $w_{-1}(n \mid n-1)(t) = K_{-n}(t)$ in HHGS scheme describe in Fig.2 (I) are defined as

$$w_1(n-1 \mid n)(t) = K_n(t) = k_1(V(t))(n_T - (n-1)),$$

and

$$w_{-1}(n \mid n-1)(t) = K_{-n}(t) = k_{-1}(V(t))n, \tag{2}$$

where $n = 1,....,4$ with $k_1(V(t)) = k_1(0)exp\left(\frac{q^+V(t)}{k_BT'}\right)$ and $k_{-1}(V(t)) = k_{-1}(0)exp\left(\frac{q^-V(t)}{k_BT'}\right)$. $q^\pm$ designates the gating charges associated with each forward and backward transition, respectively. $k_1(0)$ and $k_{-1}(0)$ are the forward and backward rate constants at zero voltage, T' is the absolute temperature and k_B is the Boltzmann constant. Now putting the transition probabilities in Eq.(1) we obtain the simplified form of the master equation as

$$\frac{dP_n(t)}{dt} = k_1(V(t))(n_T - n + 1)P_{n-1}(t) + k_{-1}(V(t))(n+1)P_{n+1}(t)$$

$$- k_1(V(t))(n_T - n)P_n(t) - k_{-1}(V(t))nP_n(t). \tag{3}$$

In this master equation, the transition probabilities are only governed by the externally applied voltage, $V(t)$. There is no influence of the diffusion of K-ions on the transition probabilities. By using this master equation, we can study the dynamics and energetics of a VGKC, where the gating-dynamics is governed in response of the voltage difference between the inside and outside of the cell.

3.2. Master equation with Diffusion

Following the classical work of Collins and Kimball(CK)[20] as well as the studies of Szabo and co-workers [21, 22], here, we have constructed the master equation for the diffusion influenced gating-process of a mutated-VGKC by considering the model described in Fig.2(2), and in this case, the master equation described in Eq.3 can be written as

$$\frac{dP_n(t)}{dt} = \alpha_{n-1}(t)P_{n-1}(t) + \beta_{n+1}(t)P_{n+1}(t) - (\alpha_n(t) + \beta_n(t))P_n(t), \tag{4}$$

where the diffusion-influenced forward transition probability, $\alpha_n(t)$ is

$$\alpha_n(t) = \frac{k_D(n_T - n)k_1(V(t))}{k_D + (n_T - n)k_1(V(t))}, \tag{5}$$

and the diffusion-influenced backward transition probability, $\beta_n(t)$ is

$$\beta_n(t) = \frac{k_D n k_{-1}(V(t))}{k_D + (n_T - n)k_1(V(t)}, \tag{6}$$

with $k_D = 4\pi DR$. R and D are the radius and the diffusion constant of a K-ion. Here it is considered that $\alpha_n(t)$ and $\beta_n(t)$ are related such a way so that at any instant of time, they follow the microscopic reversibility condition,

$$\frac{\alpha_n(t)}{\beta_{n+1}(t)} = \frac{\phi_{n+1}(t)}{\phi_n(t)} = \frac{(n_T - n)k_1(V(t))}{(n+1)k_{-1}(V(t))}, \tag{7}$$

where $\phi_n(t)$ is the invariant probability distribution, which can be expressed as

$$\phi_n(t) = \frac{\binom{n_T}{n}[\kappa(V(t))]^n}{[1 + \kappa(V(t))]^{n_T}}, \tag{8}$$

with, $\kappa(V(t)) = \left(\frac{k_1(V(t))}{k_{-1}(V(t))}\right)$. The expression of $\alpha_n(t)$ and $\beta_n(t)$ given in Eq.5 and Eq.6 are the diffusion controlled forward and backward transition probabilities of a gating process of VGKC. However, when $D \to \infty$ *i.e.*, $k_D \to \infty$, it becomes the reaction controlled situation. In this case, the second term of the denominator $(n_T - n)k_1(V(t))$ of $\alpha_n(t)$ and $\beta_n(t)$ becomes negligible compare to the first one, k_D. Therefore, at the reaction controlled limit, the expression of $\alpha_n(t)$ and $\beta_n(t)$ become

$$\alpha_n(t) = \frac{k_D(n_T - n)k_1(V(t))}{k_D} = k_1(V(t))(n_T - n)$$

$$\beta_n(t) = \frac{k_D n k_{-1}(V(t))}{k_D} = k_{-1}(V(t))n. \tag{9}$$

Therefore, in this case $\alpha_n(t)$ and $\beta_n(t)$ both becomes independent of k_D and they are similar to the expressions of the transition probabilities for the normal voltage-gated gating processes of VGKC, which are described in Eq.2 in the previous section 3.1.

3.3. Constant voltage case in presence of diffusion: an approximate solution

Traditionally the ion channel kinetics is studied using the voltage clamp technique where the voltage is varied, say from one holding potential to another by matching the voltage value to a variable control voltage[23, 24, 25]. Thereby the ion channel conductance relaxes towards its new equilibrium under a certain voltage value, say V. In the expression of α_n, as in Eq. 5, n in the denominator is replaced by n_e (equilibrium value of n). So α_n becomes

$$\alpha_n = k_1^{'}(V)(n_T - n) \tag{10}$$

where $k_1^{'}(V) = \dfrac{k_D k_1(V)}{k_D + (n_T - n_e)k_1(V)}$. Similarly, β_n is given by

$$\beta_n = k_{-1}^{'}(V)(n+1) \tag{11}$$

where $k_{-1}^{'}(V) = \dfrac{k_D k_{-1}(V)}{k_D + (n_T - n_e)k_1(V)}$.

In the constant voltage case, the solution of the master equation described in Eq.(4) is carried out by considering the detailed balance condition *i.e.,* $\alpha_{n-1}(V)P_{n-1}(t) = \beta_n(V)P_n(t)$, and it becomes a binomial probability distribution function[13, 18] given as

$$\mathrm{P_n(t)} = \frac{n_T!}{n!(n_T - n)!}[X_D(t)]^n[Y_D(t)]^{n_T - n}, \tag{12}$$

with

$$\mathrm{X}_D(t) = \frac{k_1^{'}(V)(1 - \exp(-(k_1^{'}(V) + k_{-1}^{'}(V))t))}{k_1^{'}(V) + k_{-1}^{'}(V)}, \tag{13}$$

and

$$\mathrm{Y}_D(t) = (1 - X_D(t)) = \frac{k_{-1}^{'}(V) + k_1^{'}(V)\exp(-(k_1^{'}(V) + k_{-1}^{'}(V))t)}{k_1^{'}(V) + k_{-1}^{'}(V)}. \tag{14}$$

For the solution of $P_n(t)$ for V, we assume that initially all the subunits are in inactive state, C_0 *i.e*, the $\mathrm{n} = 0$ state. Here the time dependent expression of $P_n(t)$ in Eq.(12) reveals the information about the relaxation of $P_n(t)$ with t to a equilibrium related with the voltage V. In this case, the steady state should be equilibrium, and the expression of $P_n(t)$ at equilibrium would be,

$$\mathrm{P_n^{eq}} = \frac{n_T!}{n!(n_T - n)!}[X_D^{eq}]^n[Y_D^{eq}]^{n_T - n}, \tag{15}$$

with $X_D^{eq} = \dfrac{k_1^{'}(V)}{k_1^{'}(V) + k_{-1}^{'}(V)}$ and $Y_D^{eq} = \dfrac{k_{-1}^{'}(V)}{k_1^{'}(V) + k_{-1}^{'}(V)}$.

The average number of subunits in active state is expressed as $\langle n \rangle(t) = n_T X_D(t)$ and the average number of subunits in inactive state is $\langle n_T - n \rangle(t) = n_T Y_D(t)$. The parameter $\mathrm{X}_D(t)$ satisfies the differential equation[3, 18]

$$\frac{\mathrm{dX_D(t)}}{\mathrm{dt}} = k_1^{'}(V)(1 - X_D(t)) - k_{-1}^{'}(V)(X_D(t)). \tag{16}$$

This equation is similar to the equation for the open state probability, originally introduced by Hodgkin and Huxley to model the potassium ion channel conductance [3, 18, 13], Here we have re-established this expression for the diffusion influenced gating processes of a VGKC. However, the equilibrium probability of the ion-conducting state[23] does not change for the diffusion influenced and without diffusion influenced cases, and appears as the Boltzmann distribution of power n_T,

$$\mathrm{P}_{n_T}^{(eq)} = \left[\frac{1}{1+K_{eq}(0)exp\left(\frac{-q(V)}{k_B T'}\right)}\right]^{n_T}, \tag{17}$$

with $q = (q^+ - q^-)$ and $K_{eq}(0)$ is the equilibrium constant defined as $K_{eq}(0) = \left(\frac{k_{-1}(0)}{k_1(0)}\right)$, which is independent of diffusion constant.

3.4. Effect of Diffusion for continuous time-periodic voltage

Here we describe the kinetics of a single mutated VGKC for continuous time periodic voltage based on the diffusion influenced gating scheme depicted in Fig.2 (2). To get some analytical understanding, we have expressed the overall VGKC-dynamics in terms of the open state probability $P_4(t)$, and the rate-expression can be written from Eq.(4) as

$$\frac{dP_4(t)}{dt} = \alpha_3(t)P_3(t) - \beta_4(t)P_4(t). \tag{18}$$

By using the normalization condition $\sum_{n=0}^{4} P_n(t) = 1$, we can rewritten Eq.(18) as

$$\frac{dP_4(t)}{dt} = \chi_D(t) - K_D(t)P_4(t), \tag{19}$$

where $\chi_D(t) = \alpha_3\left[1-\{P_0(t)+P_1(t)+P_2(t)\}\right]$ and $K_D(t) = \left[\alpha_3+\beta_4\right]$. Here $\alpha_n(t)$ and $\beta_n(t)$ depends on the diffusion coefficient as defined in Eq. (5) and (6). This ensures that in the low frequency limit $P_4^{(ss)}(t)$ in Eq.48 becomes

$$P_4^{(ss)}(t) = \frac{\chi_D(t)}{K_D(t)}, \tag{20}$$

and in high frequency limit, it becomes in Eq.(52) as

$$P_4^{(ss)}(t) = \frac{\langle\chi_D(t)\rangle}{\langle K_D(t)\rangle}. \tag{21}$$

For more detailed understanding see Appendix. Here the superscript (SS) indicates the time-periodic steady state. One must also note that although the equations (20) and (21) give the steady state ion-conducting probability, $P_4^{(ss)}(t)$ in compact form, it is not possible to evaluate analytically as $\chi(t)$ depends on $P_0(t), P_1(t)$ and $P_2(t)$. To determine these probabilities, we resort to numerical solution of the master equation described in Eq.(4) with time-dependent transition probabilities for oscillating voltage. The numerically determined time-dependent probabilities, $P_n(t)$ are used to obtain the ionic current and entropy production rates for further studies.

3.5. Entropy production rates as nonequilibrium response characteristics

Here we discuss the isothermal nonequilibrium energetics of a mutated VGKC through the various entropy production rates. Starting from the definition of the entropy of a system in terms of the Gibbs entropy

$$S_{sys}(t) = -k_B \sum_n P_n(t) \ln P_n(t), \tag{22}$$

we get the system entropy production rate (epr) as

$$\dot{S}_{sys}(t) = \sum_n \left[\alpha_{n-1}(t)P_{n-1}(t) - \beta_n(t)P_n(t)\right] \times \ln\left[\frac{P_{n-1}(t)}{P_n(t)}\right], \tag{23}$$

where the entropy production is given in the unit of Boltzmann constant, k_B. Here the system should be the gating-dynamics of a VGKC. The voltage-dependent transition probabilities are function of time due to the explicit time-dependence of the voltage. The system epr can be split as

$$\dot{S}_{sys}(t) = \dot{S}_{tot}(t) - \dot{S}_m(t), \tag{24}$$

where the first term in the r.h.s. of Eq.(24) gives the total epr and the second term denotes the medium epr due to the entropy flux into the surroundings. The expression of the total and medium eprs can be expressed as

$$\dot{S}_{tot}(t) = \sum_n \left[\alpha_{n-1}(t)P_{n-1}(t) - \beta_n(t)P_n(t)\right] \times \ln\left[\frac{\alpha_{n-1}(t)P_{n-1}(t)}{\beta_n(t)P_n(t)}\right], \tag{25}$$

and

$$\dot{S}_m(t) = \sum_n \left[\alpha_{n-1}(t)P_{n-1}(t) - \beta_n(t)P_n(t)\right] \times \ln\left[\frac{\alpha_{n-1}(t)}{\beta_n(t)}\right], \tag{26}$$

where we have considered the boundary conditions $P_{n-1} = 0$ for $n = 0$ and $P_{n+1} = 0$ for $n = n_T$. For constant voltage, $\alpha_n(t)$ and $\beta_n(t)$ should be a function of a fixed voltage value, V, whereas, for oscillating voltage, the transition probabilities should be dependent on the time periodic voltage value, $V(t)$ at time t. The expressions of $\dot{S}_{tot}(t)$, $\dot{S}_m(t)$ and $\dot{S}_{sys}(t)$ help us in explaining the diffusion influenced non-equilibrium energetics of a VGKC at constant as well as the oscillating voltage cases, which we will thoroughly discuss in the numerical section.

3.6. Factors governing the nonequilibrium dynamics of a VGKC: an energetic view point

To study whether the diffusion-influenced non-equilibrium VGKC-dynamics is free-energy or entropy driven, here we have calculated the change of total internal energy $\Delta U(t)$, the free energy change, $\Delta F(t)$, and the change of system entropy $\Delta S_{sys}(t)$. The changing of these thermodynamic quantities have been measured with respect to their equilibrium values at any instant of time t. For pursuing our analysis, we have considered the total internal energy of the non-equilibrium VGKC-dynamics at time t as

$$U(t) = -T \sum_i P_i(t) \ln \phi_i(t), \tag{27}$$

the system entropy production,

$$S_{sys}(t) = -\sum_i P_i(t) \ln P_i(t), \tag{28}$$

and thereby the free energy as

$$F(t) = U(t) - TS(t) = T \sum_i P_i(t) \ln\left(\frac{P_i(t)}{\phi_i(t)}\right). \tag{29}$$

Here, $\phi_i(t)$ is the invariant probability distribution, which obeys the microscopic reversibility condition at any time t. In this time-dependent non-equilibrium thermodynamics, this reversibility condition provides the equilibrium information of the system corresponding to the voltage value, $V(t)$ at time t. With changing time from $t \to t'$, the voltage value will be changed from $V(t) \to V(t')$. As a consequence, the equilibrium information would be changed as the system will attain a new equilibrium state corresponding the voltage value $V(t')$ at time t'. Now we have defined $\frac{\Delta U(t)}{T}$, $\frac{\Delta F(t)}{T}$ ΔS as,

$$\frac{\Delta U}{T} = \frac{U^e(t)}{T} - \frac{U(t)}{T} = \sum_i (P_i(t) - \phi_i(t)) \ln \phi_i(t) \tag{30}$$

where

$$U^e = -T \sum_i \phi_i(t) \ln \phi_i(t). \tag{31}$$

Similarly we can write,

$$\frac{\Delta F}{T} = \frac{F^e}{T} - \frac{F(t)}{T} = -\frac{F(t)}{T} = -\sum_i P_i(t) \ln\left(\frac{P_i(t)}{\phi_i(t)}\right) \tag{32}$$

and

$$\Delta S = \frac{\Delta U}{T} - \frac{\Delta F}{T}. \tag{33}$$

This analysis will help us in understanding how much internal energy, free-energy or system entropy would be changed if a system goes from the equilibrium to the non-equilibrium state due to an external time-dependent perturbation. In this system, the external time-dependent perturbation is the time-periodic oscillating voltage. Here we choose these three thermodynamic quantities as all of them are the state function.

4. Numerical study of Kinetics and Thermodynamics with diffusion

In this section, we have numerically studied the effect of diffusion on the mutated VGKC-dynamics as well as its energetics for the constant and time-dependent oscillating voltage. We have considered the rate parameters[16] on the *Shaker* potassium ion channel expressed in mammalian cells, tsA 201. The rate constants at zero voltage are $k_1(0) = 124.8 s^{-1}$ and $k_{-1}(0) = 4.74 s^{-1}$. The gating charges associated with each forward and backward transitions rates are $q^+ = 0.66e$ and $q^- = -0.64e$, respectively at temperature $12^0 C$.

Now, before going into the details about our numerical illustrations, we want to clarify that in our numerical analysis, the K-ionic current is designated the current, whose origin is due to the diffusion of K-ions through the CICP, opened when all the sub-units remain in the active conformation. Generally, the K-ionic current is calculated as

$$I(t) = g_0 \times g(V(t)) \times (V(t) - V_r) P_4(t), \tag{34}$$

where g_0 is the overall scaling factor representing the cell expression rate[16, 17] taken as $g_0 = 1.013$ and the functional form of the nonlinear conductance [17], $g(V(t))$ (in microSiemens, μS) is taken as $g(V(t)) = 1.340 \times 10^{-9} (V(t))^3 - 7.30 \times 10^{-8} (V(t))^2 - 3.35 \times 10^{-5} (V(t)) + 4.470 \times 10^{-3}$. $V_r = -90 mV$ is the reversal potential at which no K-ionic current would be obtained. In our study, we have not calculated any ω-current which can be obtained due to diffusion of the K-ions through the mutated VSD. Here our interest lies in

studying the effect of K-ionic diffusion on the gating-mechanism of a VGKC, and for that, we have proposed our diffusion influenced gating scheme described in Fig.2(2).

4.1. Constant voltage Case

In constant voltage case, we have provided the kinetic description in terms of the K-ionic current, $\mathrm{I}(t)$ which is calculated according to the Eq.(34), where $V(t)$ is not a function of time, rather it becomes a fixed voltage value, V .

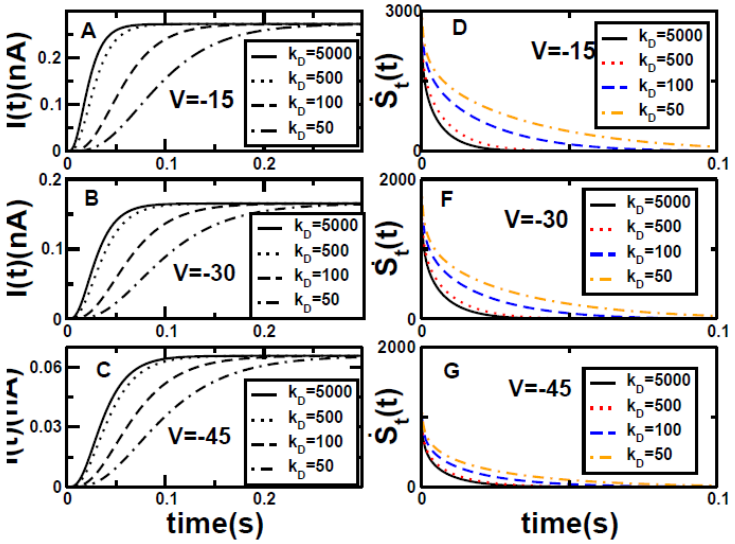

Figure 3: (A),(B),(C) Ionic current, $\mathrm{I}(t)$ in nanoAmpere(nA) is plotted against time (in s) at constant depolarizing voltages, V=-15,-30 and -45 mV, respectively for $k_D = 5000,500,100,50$. In (D), (E) and (F), the total entropy production rate(epr), $\dot{S}_{tot}(t)$ or $\dot{S}_t(t)$ is plotted as a function of time at depolarizing voltages, V=-15, V=-30 and -45 mV, respectively for $k_D = 5000,500,100,50$.

Now to study the effect of k_D (diffusion) on the ionic current, here in Fig. 3(A),(B),(C) we have plotted $I(t)$ as a function of time for three constant voltage values $V = -15$, $V = -30$ and $V = -45$, respectively. The common trend among all of these curves is that I(t) first increases with time and then saturates at a constant value. However, the magnitude of I(t) increases with increase in the constant (depolarizing) voltage value. In each of these figures, we have varied the values of k_D from 5000 to 50. When $k_D = 5000$, it is the reaction controlled limit where diffusion has no influence on the gating mechanism. But as k_D decreases from 500 to 50, the effect of k_D is more pronounced, where the ionic current $I(t)$ reaches its saturation value at a much later time as the value of k_D decreases. The result indicates that the diffusion of K-ions through VSD delays the gating-mechanism in opening the K-channel pore.

To investigate the thermodynamics of the diffusion-influenced gating-mechanism at constant voltage, we have calculated the total entropy production rate, $\dot{S}_{tot}(t)$. Substituting the time-dependent probability value, $P_n(t)$ from Eq.(12), we obtain

$$\dot{S}_{tot}(t) = \left[k_1(V)\langle n_T - n(t)\rangle - k_{-1}(V)\langle n(t)\rangle\right] \times ln\left[\frac{k_1(V)Y_D(t)}{k_{-1}(V)X_D(t)}\right]. \quad (35)$$

In Fig.3(D),(E),(F) we have plotted $\dot{S}_{tot}(t)$ as a function of time for different k_D values at $V=-15,-30$ and $-45mV$, respectively. The value of $\dot{S}_{tot}(t)$ at a particular time is higher for higher value of V. For a particular value of V, the value of $\dot{S}_{tot}(t)$ at earlier times becomes lower as the value of k_D decreases from 5000 to 50. After a certain time there is a crossover after which the curve for lower k_D has higher value and goes to zero at a much later time indicating that the gating-dynamics reaches equilibrium. Mathematically, we can also understand that why $\dot{S}_{tot}(t)$ becomes zero at equilibrium for constant voltage. This can be shown if we use the steady state (equilibrium) values of $X_D(t)$ and $Y_D(t)$, $\mathrm{X}^{(eq)}=\left(\frac{k_1(V)}{k_1(V)+k_{-1}(V)}\right)$ and $\mathrm{Y}^{(eq)}=\left(\frac{k_{-1}(V)}{k_1(V)+k_{-1}(V)}\right)$, respectively (see section 3.3) into Eq.(35) , then we can observe that $\dot{S}_{tot}(t)$ becomes zero at equilibrium for a constant external voltage.

4.2. Effect of Diffusion on Dynamic hysteresis behaviour for oscillating Voltage

For pursuing our study, here, we have considered a time-dependent sinusoidal voltage variation, $V(t)=V_0+V_a sin\omega t$ with mean V_0, amplitude V_a and frequency ω. We numerically solve the master equation in Eq.4 to get the probabilities of all the Markov states in the diffusion influenced five-state Hodgkin Huxley type gating scheme, depicted in Fig.2(2). The ionic current, $I(t)$ and various entropy production rates are then determined by using these probability values. In Fig.4, we observe that for oscillating external voltage, the ionic current, $I(t)$ as well as total epr, $\dot{S}_{tot}(t)$ reaches a time-periodic steady value. The time periodic steady values of $I(t)$ and $\dot{S}_{tot}(t)$ are designated as $I^{(ss)}(t)$ and $\dot{S}_{tot}^{(ss)}(t)$, respectively. Here we observe that the steady state of the diffusion influenced gating process is actually a nonequilibrium steady state(NESS), characterized by the non-zero values of $\dot{S}_{tot}(t)$. Moreover, In Fig. 4(A),(B) and (C), $I(t)$ is plotted as a function of time for several values of k_D for low ($\omega/2\pi=0.1Hz$), medium ($\omega/2\pi=100$ Hz), and high ($\omega/2\pi=5000$ Hz) frequency values. We observe that as the value of k_D decreases, the current reaches its saturation value at a much later time indicating the diffusion influenced delayed in the conduction of K-ions due to decreasing the probability of opening the central ion conducting pore (CICP). This observation is similar for the constant voltage cases. Furthermore, we can also observe that as k_D decreases, the depth of oscillation in the current curve decreases significantly for $\omega/2\pi=100$ and 5000 Hz at extreme diffusion limit ($k_D=50$). However, at low frequency, $\omega/2\pi=0.1$ Hz, this phenomenon is absent. Similarly, to investigate whether such phenomenon is present in the thermodynamic quantities or not, here, in Fig.4 (D),(E) and (F), the total epr is plotted for these three frequency values. We observe that the decreasing of the depth of oscillation is not so pronounced for $\dot{S}_{tot}(t)$ like in $I(t)$ for these medium and high frequency values for $k_D=50$. Moreover, in this case, we observe that for a particular frequency, the value of $\dot{S}_{tot}(t)$ is lower for lower value of k_D at transient times, however, after a certain time there is a cross over for the curves of $\dot{S}_{tot}(t)$ and the curves go to zero at much later time for lower k_D values.

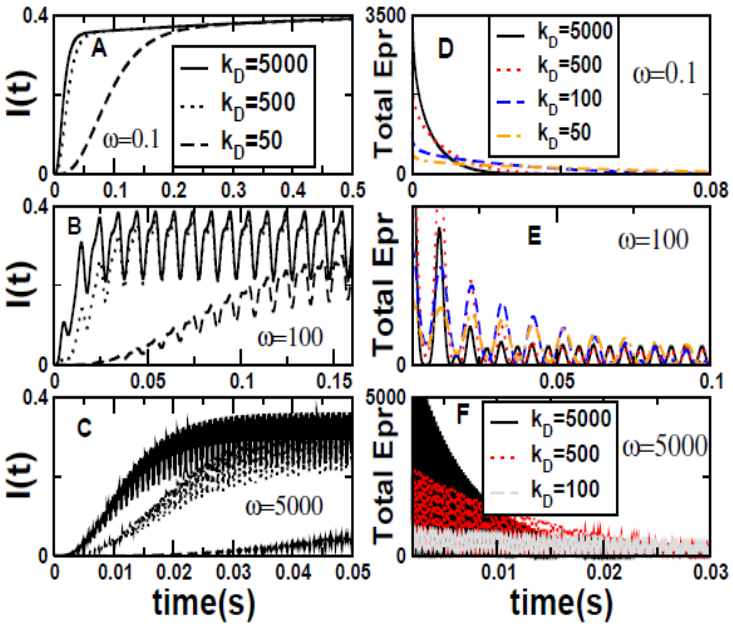

Figure 4: The ionic current, $I(t)$ *and entropy production rate,* $\dot{S}_{tot}(t)$ *or* $\dot{S}_t(t)$ *are plotted as a function of time for* $k_D = 5000,500,50$.

For more understanding about the consequences of the decreasing of the depth of oscillation, $I^{(ss)}(t)$ vs voltage and $P_4^{(ss)}(t)$ vs voltage are plotted for low, medium and high frequency values of the external voltage at steady state over a period. The dynamic hysteresis phenomena is observed where the hysteresis loop area tends to vanish at very low and at very high frequencies. This phenomena has been already reported in our previous study[13]. However, here, our main motivation is to describe the effect of diffusion on that hysteresis loop area. For that, in Fig.5(A),(B),(C) we have plotted $I^{(ss)}(t)$ as a function of voltage for different k_D values. At very low frequency $(\omega/2\pi = 0.1)$ Hz the effect of k_D is almost negligible. However, at medium frequency, $(\omega/2\pi = 100)$ Hz the effect of k_D is more pronounced. When the value of k_D is 5000 *i.e.,* at reaction controlled limit, the hysteresis loop area is maximum. But with decreasing the value of k_D the loop area also decreases, until k_D value goes to below 50. At high frequency $(\omega/2\pi = 5000)$, the loop is not noticeable, but the effect of k_D is observed for the significant changing in magnitude of $I^{(ss)}(t)$. The change of the magnitude is nonlinear and deceases with decreasing in the value of k_D. Now, the dynamic hysteresis is a non-equilibrium phenomena which signifies the memory developed due to dynamics of a system. From this curves, we can conclude that in the non-equilibrium VGKC-dynamics, the diffusion of K-ions through VSD try to destroy the memory, which is developed due to the K-ionic conduction through the CICP at frequency $(\omega/2\pi = 100)$ Hz. As ionic current, $I(t)$ mainly depends on the open state probability, $P_4(t)$, so for finding out the origin about this phenomena, here, in Fig.5 (D), (E), (F) we have plotted $P_4^{(ss)}(t)$ vs voltage for low , medium and high frequency values to study the effect of k_D. From the observation of these curves we can conclude that $P_4^{(ss)}(t)$ is mainly responsible for which $I^{(ss)}(t)$ shows this type of behaviour.

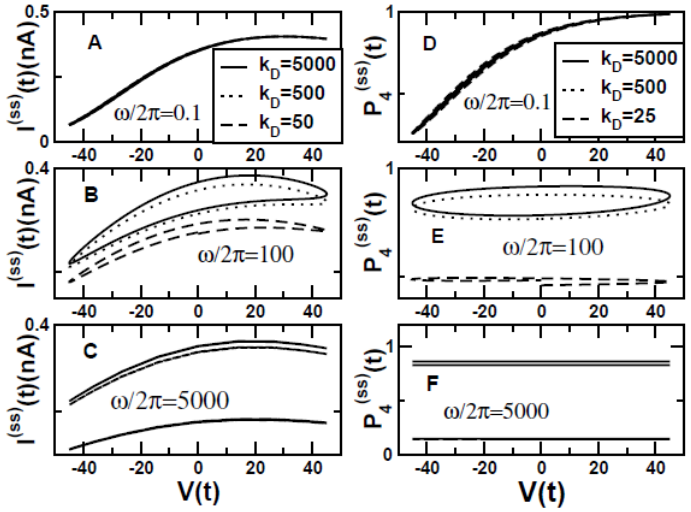

Figure 5: In figures (A),(B) and (C), ionic current, $I^{(ss)}(t)$ *, is plotted against oscillating voltage (sinusoidal) with frequency* $\omega/2\pi = 0.1,100.0$ *and* 5000.0 *Hz, respectively at NESS over a time period for* $k_D = 5000,500,50$ *. In figures (D),(E) and (F) probability of ion conducting state,* $P_4^{(ss)}(t)$ *, is plotted against oscillating voltage (sinusoidal) with frequency* $\omega/2\pi = 0.1,100.0$ *and* 5000.0 *Hz, respectively at NESS over a time period for* $k_D = 5000,500,25$.

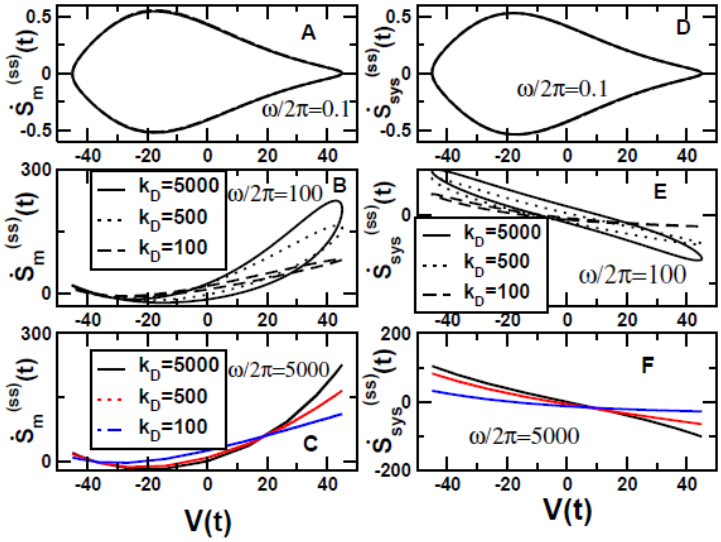

Figure 6: In figures (A),(B) and (C), medium entropy production rate, $\dot{S}_m^{(ss)}(t)$ *is plotted against oscillating voltage (sinusoidal) with frequency* $\omega/2\pi = 0.1,100.0$ *and* 5000.0 *Hz, respectively at NESS over a time period for* $k_D = 5000,500,100$. *In figures (D), (E) and (F) system entropy production rate,* $\dot{S}_{sys}^{(ss)}(t)$ *is plotted against oscillating voltage (sinusoidal) with frequency* $\omega/2\pi = 0.1,100.0$ *and* 5000.0 *Hz, respectively at NESS over a time period for* $k_D = 5000,500,100$.

Next we have investigated such behaviour in the non-equilibrium thermodynamic properties of a VGKC-dynamics. For pursuing our analysis, $\dot{S}_m^{(ss)}(t)$ vs $V(t)$ is plotted in Fig.6(A),(B) and (C) for the frequency values

$\omega/2\pi = 0.1,100$ and 5000 Hz, respectively. The similar type of plots have been carried out for $\dot{S}_{sys}^{(ss)}(t)$ vs $V(t)$ for these three frequency values, which are depicted in Fig.6(D),(E) and (F). The other thermodynamic quantity, $\dot{S}_{tot}^{(ss)}(t)$ is also plotted as a function of $V(t)$ for the low, medium and high frequencies in Fig.7 (a), (b) and (C). These curves infer that at $\omega/2\pi = 100$ Hz, the dynamic hysteresis loop area of $\dot{S}_{m}^{(ss)}(t)$ vs $V(t)$, $\dot{S}_{sys}^{(ss)}(t)$ vs $V(t)$ and $\dot{S}_{tot}^{(ss)}(t)$ vs $V(t)$ curves are annihilated in the influence of the diffusion of K-ions, which is similar with the results obtained from the plot of $I^{(ss)(t)}$ versus $V(t)$ in Fig.5. Therefore, from the study of the kinetic and thermodynamic properties of the VGKC-dynamics, we can make a conclusion that the diffusive motion of the K-ions through a mutated VGKC has a natural tendency in destroying the dynamic hysteresis behaviour of a VGKC at non-equilibrium.

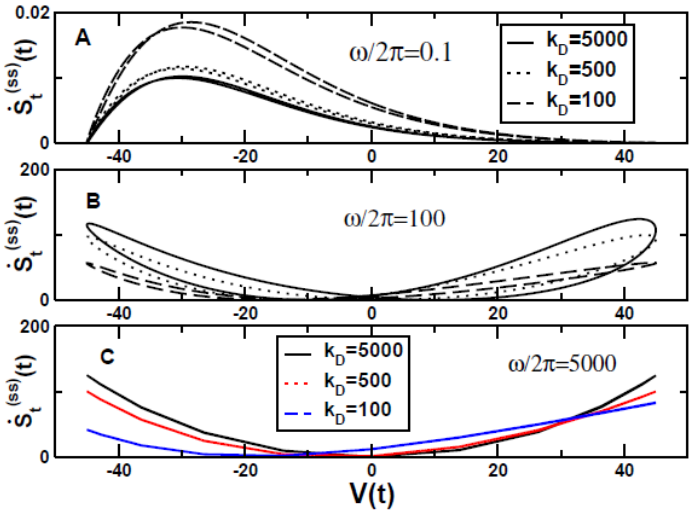

Figure 7: Total entropy production rate, $\dot{S}_{tot}^{(ss)}(t)$ or $\dot{S}_{t}(t)$ is plotted against oscillating voltage, $V(t)$ at low, medium and high frequency values at steady state over a time period which are depicted in figures (A), (B) and (C), respectively for $k_D = 5000,500,100$.

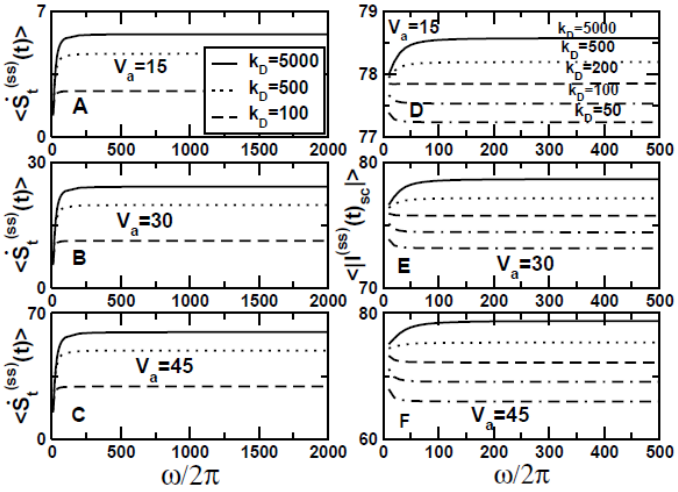

Figure 8: In figures (A),(B),(C) Average entropy production rate over a period, $\langle \dot{S}_{tot}^{(ss)}(t) \rangle$ or $\dot{S}_{t}(t)$ is plotted against frequency, $\omega/2\pi$ with amplitude, $V_a = 15,30,45$ mV for $k_D = 5000,500,100$. In figures (D),(E),(F)

$\langle [I^{(ss)}(t)]_{sc} \rangle$ *indicates the ionic current over a period scaled with* $g(v)$ *and is plotted against frequency,* $\omega/2\pi$ *with the same amplitudes. With increasing the amplitude values and* k_D *values.*

Then the average total epr over a time period, $\langle \dot{S}_{tot}^{(ss)}(t) \rangle$ is shown at NESS as a function of the frequency of the external voltage. Here the average is defined as $\langle \dot{S}_{tot}^{(ss)}(t) \rangle = \frac{1}{T}\int_0^T \dot{S}_{tot}^{(ss)}(t)dt$. One can see that the average total epr increases steadily from zero at very low frequency and saturates at high frequency values. Therefore, the nonequilibrium steady state reached by the system is infinitesimally close to equilibrium at the $\omega \to 0$ limit whereas it is farthest from equilibrium at the $\omega \to \infty$ limit for the given parameters of the model system and the amplitude of the external voltage. In Fig.8(A),(B),(C) we have plotted $\langle \dot{S}_{tot}^{(ss)}(t) \rangle$ against frequency for three different values of amplitude. As the value of k_D decreases, the magnitude of $\langle \dot{S}_{tot}^{(ss)}(t) \rangle$ decreases in all the three cases. The nature of the curve remains same essentially, however, the value of $\langle \dot{S}_{tot}^{(ss)}(t) \rangle$ increases for the higher values of the amplitude of $V(t)$

The average current over a period, $\langle [I^{(ss)}(t)]_{sc} \rangle$ are then studied as a function of frequency at different voltage amplitudes. Here the 'sc' superscript indicates that the ionic current is scaled with the nonlinear conductance, g(V). The functional form of $g(V)$ is generally an experimentally determined equation that can vary from experiment to experiment. So to obtain the general behavior of the ionic current we have calculated the scaled current. It is observed that the average ionic current, $\langle [I^{(ss)}(t)]_{sc} \rangle$ increases to saturation with increase in the frequency value. In the high frequency limit, $\langle [I^{(ss)}(t)]_{sc} \rangle$ becomes almost independent of amplitude. But as the value of k_D decreases, the trend is reversed. For values of k_D lower than 100 the ionic current $\langle [I^{(ss)}(t)]_{sc} \rangle$ decreases with increasing frequency and becomes constant for higher frequencies. The trend remains same for all the three values of amplitude.

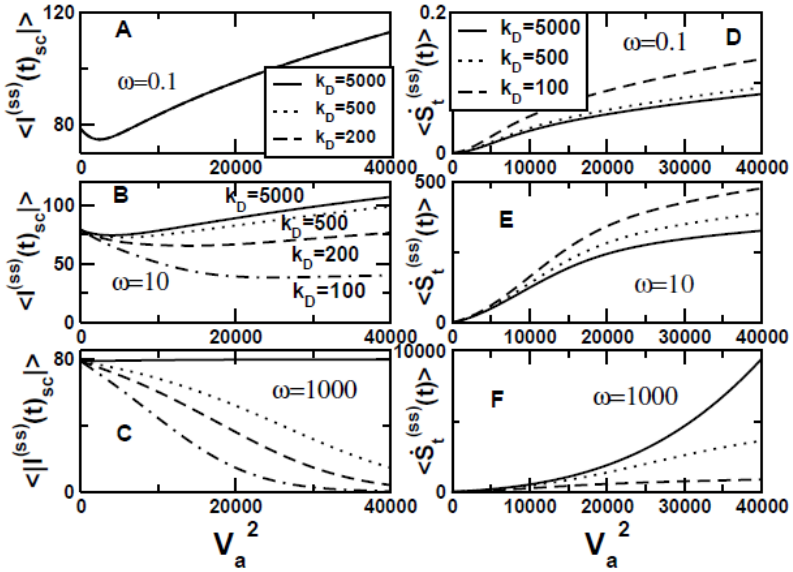

Figure 9: In figures (A),(B) and (C), average Ionic current over a period at steady state, $\langle [I^{(ss)}(t)]_{sc} \rangle$ *is plotted against square of the amplitude,* V_a^2 *at low (* $\omega/2\pi = 0.1$ *Hz), medium (* $\omega/2\pi = 10$ *Hz) and high frequency (*

$\omega/2\pi = 1000$ Hz), respectively for different values of k_D. Average entropy production rate over a period at steady state, $\langle \dot{S}_{tot}^{(ss)}(t) \rangle$ or $\dot{S}_t(t)$ is plotted against V_a^2 with the same frequency values which are depicted in (D),(E) and (F), respectively.

To understand the amplitude dependence of $\langle [I^{(ss)}(t)]_{sc} \rangle$ and $\langle \dot{S}_{tot}^{(ss)}(t) \rangle$ for the mutated VGKC-dynamics, here these two quantities are plotted as a function of V_a^2 for low, medium and high frequency values at NESS shown in Fig.9. For oscillating voltage, V_a^2 is proportional to the energy supplied to the system and $\dot{S}_{tot}(t)$ is a measure of the dissipative flux from the system. In Fig.9 (A) and (D), $\langle [I^{(ss)}(t)]_{sc} \rangle$ and $\langle \dot{S}_{tot}^{(ss)}(t) \rangle$ are plotted as a function of V_a^2 at low frequencies $\omega/2\pi = 0.1$ Hz, where we observe that in Fig.9 (A), $\langle [I^{(ss)}(t)]_{sc} \rangle$ increases with increasing the value of V_a^2 after passing through a minimum. Such behavior is generated due to the determination of the current from Eq.(34). In this case, k_D has no effect on $\langle [I^{(ss)}(t)]_{sc} \rangle$, whereas with increasing the value of V_a^2, $\langle \dot{S}_{tot}^{(ss)}(t) \rangle$ first increases and then reaches a saturated value which is shown in Fig.9 (D). In this case, $\langle \dot{S}_{tot}^{(ss)}(t) \rangle$ increases with decreasing the values of k_D. At medium frequency limit, $\omega/2\pi = 10$ Hz, the tendency of $\langle [I^{(ss)}(t)]_{sc} \rangle$ in passing through a minimum, vanishes. In this case, we observe that at reaction controlled limit $k_D = 5000$, $\langle [I^{(ss)}(t)]_{sc} \rangle$ increases slightly with increasing the values of V_a^2, but with decreasing the values of k_D *i.e.*, at diffusion controlled limit, $\langle [I^{(ss)}(t)]_{sc} \rangle$ decreases with k_D until it reaches a steady value at higher V_a which is shown in Fig.9(B). For $\langle \dot{S}_{tot}^{(ss)}(t) \rangle$, we see that at $\omega/2\pi = 10$ Hz, its values as a function of V_a^2 first increases and then get saturated which is shown in Fig.9(E). Here, with decreasing the values of k_D, $\langle \dot{S}_{tot}^{(ss)}(t) \rangle$ increase at higher values of V_a^2. At high frequency, $\omega/2\pi = 1000$ Hz, $\langle [I^{(ss)}(t)]_{sc} \rangle$ remains constant with the variation of V_a^2 at reaction controlled limit ($k_D = 5000$), but with decreasing the values of k_D, $\langle [I^{(ss)}(t)]_{sc} \rangle$ decreases nonlinearly with V_a^2, which is depicted in Fig.9(C). In this case, $\langle [I^{(ss)}(t)]_{sc} \rangle$ decreases more rapidly with V_a^2 compare to the trend observed in Fig.9(B). However, in this frequency range ($\omega/2\pi = 1000$ Hz), $\langle \dot{S}_{tot}^{(ss)}(t) \rangle$ increases exponentially with V_a^2 at reaction controlled limit, and the trend of the variation of $\langle \dot{S}_{tot}^{(ss)}(t) \rangle$ as a function of V_a^2 with k_D is totally reverse in comparison with the low and medium frequency cases, where in the high frequency, we observe that $\langle \dot{S}_{tot}^{(ss)}(t) \rangle$ decreases with decreasing the values of k_D which is shown in Fig.9(F). Now from the above discussion, we can find a inverse relation between the variation of $\langle [I^{(ss)}(t)]_{sc} \rangle$ and $\langle \dot{S}_{tot}^{(ss)}(t) \rangle$ with V_a^2 at reaction controlled limit. We observe that with increasing the frequency values, $\langle [I^{(ss)}(t)]_{sc} \rangle$ gets saturation, and becomes independent of V_a^2 *i.e.*, the input energy, whereas, $\langle \dot{S}_{tot}^{(ss)}(t) \rangle$ increases non-linearly with V_a^2. However, diffusion destroy such relation between $\langle [I^{(ss)}(t)]_{sc} \rangle$ and $\langle \dot{S}_{tot}^{(ss)}(t) \rangle$.

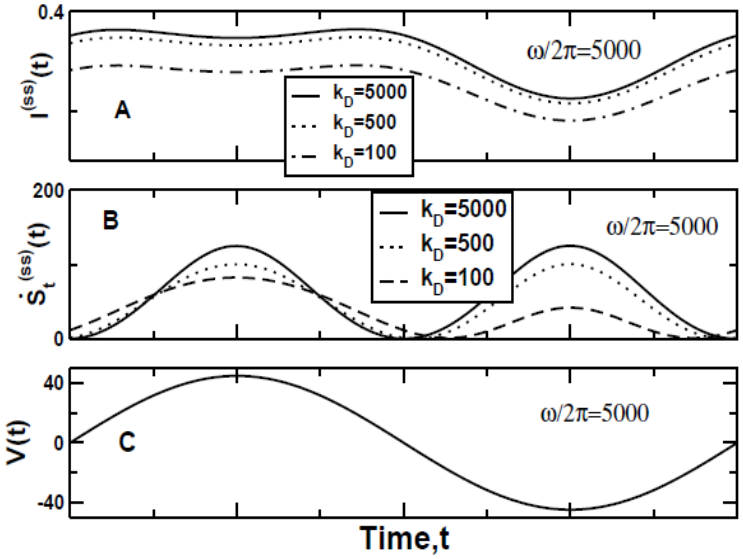

Figure 10: The ionic current, $I^{(ss)}(t)$*, total entropy production rate,* $\dot{S}_{tot}^{(ss)}(t)$ *or* $\dot{S}_t(t)$ *and oscillating voltage,* $V(t)$ *are plotted with time at* $\omega/2\pi = 5000Hz$ *over an oscillation period at NESS. Time required to complete an oscillation cycle is same for* $I^{(ss)}(t)$ *but half for* $\dot{S}_{tot}^{(ss)}(t)$ *compared to that of voltage* $V(t)$.

Next, we report an another intriguing observation in Fig.10. Here, the ionic current, $I^{(ss)}(t)$, the total entropy production rate, $\dot{S}_{tot}^{(ss)}(t)$ and $V(t)$ are plotted at high frequency, $\omega/2\pi = 5000Hz$ over a period at steady state in Fig.10 (A), (B) and (C), respectively. It is observed that in the high frequency regime, $\dot{S}_{tot}^{(ss)}(t)$ oscillates with a time period which is half of the external voltage, $V(t)$. However, the time period of ionic current, $I^{(ss)}(t)$ is the same as that of the external voltage. Hence at the high frequency limit, the total epr at NESS oscillates with a frequency which is double of that of the external voltage. For the $I^{(ss)}(t)$ plot the value of ionic current decreases with the decrease in value of k_D. The nature of the curve remains unchanged. For the plot of $\dot{S}_{tot}^{(ss)}(t)$, the symmetry of the curve is lost due to the effect of k_D. The magnitude of the curve decreases with the decrease in value of k_D. The centre of the curve also shifts to the right.

In Fig.11(A), (B) and (C), the change in free energy $\frac{\Delta F}{T}$, internal energy $\frac{\Delta U}{T}$ and entropy ΔS are plotted against time for $k_D = 5000,500$ and 50, respectively for a constant voltage $V = -15$ mV. The same plot has been carried out in Fig.12 for an oscillating voltage $V(t)$. In both cases, *i.e.*, constant and oscillating voltage cases, it is observed that for low value of $k_D = 50$ *i.e.,* at diffusion controlled limit, the reaction is entropy driven initially as well as finally. However, at diffusion controlled limit, *i.e.,* $k_D = 5000$, the reaction is initially entropy driven and finally it becomes internal energy driven. Intermediate behaviour is seen for intermediate values of k_D.

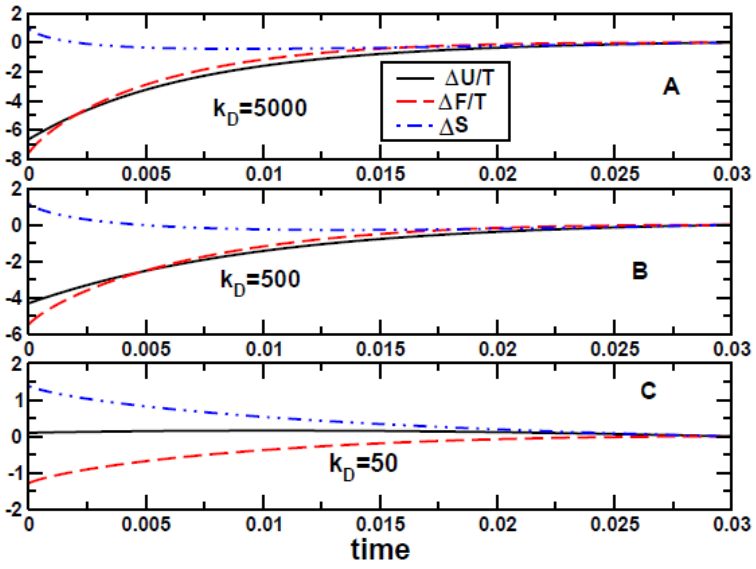

Figure 11: The change in free energy $\frac{\Delta F}{T}$, *internal energy* $\frac{\Delta U}{T}$ *and entropy* ΔS *is plotted against time for* $k_D = 5000,500,50$, *for a constant voltage* $V = -15$.

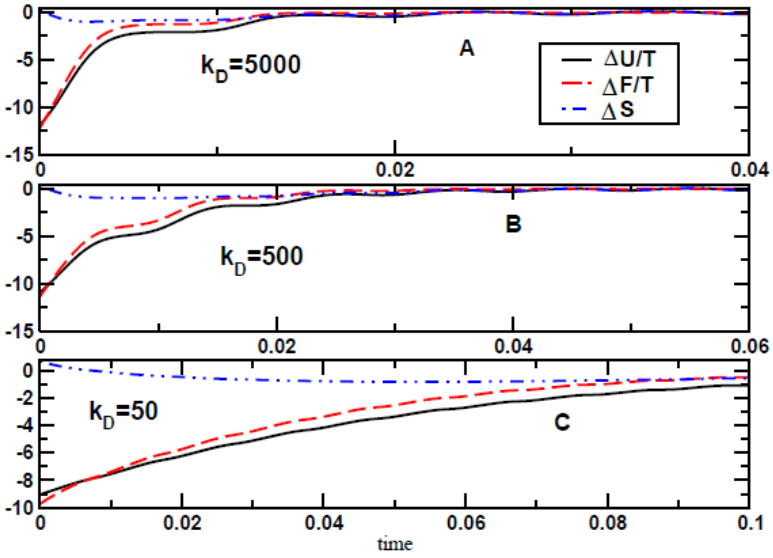

Figure 12: The change in free energy $\frac{\Delta F}{T}$, *internal energy* $\frac{\Delta U}{T}$ *and entropy* ΔS *is plotted against time for* $k_D = 5000,500,50$, *for an oscillating voltage* $V(t)$.

5. Conclusion

Here we have studied the diffusion influenced non-equilibrium dynamics as well as its energetics of a single VGKC. To understand how the diffusion of the K-ions affect the VGKC- dynamics, here we have proposed a diffusion influenced five-state Hodgkin-Huxley type gating scheme where it is considered that the K-ions can also diffuse through the voltage-sensing domain. The important points of the work are given below.

(1) We have incorporated this idea of the permeation of K-ions through VSD according to the molecular-dynamic study of Khalili-Araghi *et al.*, where they have shown that even when the central ion-conducting pore remains closed, the diffusion of K-ions is possible through a mutated VSD, which results the ω-current.

(2) To study the diffusion influenced dynamics as well as the energetics of the non-equilibrium VGKC-gating, here we have constructed the corresponding master equation where it is considered that the channel protein is continuously excited by the oscillating voltage so that the channel protein is compelled to show its non-equilibrium response far away from equilibrium.

(3) For complete study, we have pursued our analysis for constant voltage case, where it is shown that the single parameter Hodgkin Huxley equation is related to the master equation for the transition between the five conformational states even in presence of diffusion.

(4) Both for constant and oscillating voltage, we have observed that at diffusion controlled limit, the gating process becomes delayed and as a consequence, the ionic current takes more time to reach its steady value compared to that of the reaction controlled limit.

(5) At the medium frequency range of the oscillating voltage, it is observed that the diffusion of the K-ions diminishes the dynamic hysteresis loop areas, shown in the plots of the ionic current as well as total, medium and system entropy production rates with the voltage.

(6) Moreover, for oscillating voltage the diffusion time scale interferes with the intrinsic time scale of the ion-channel producing a beating phenomenon in the current signal whose modulation depth depends on the diffusion rate. This modulation of interference beat can be utilized dynamically to control over any other time scale, for example, drug binding rate or other externally controlled rate process.

(7) At reaction controlled limit, the ionic current and the total entropy production rate i.e., the total dissipation rate obeys the inverse relation with the square of the amplitude, of the oscillating voltage, however, at diffusion controlled limit, such relation is broken down.

(8) Another intriguing observation is that at extreme high frequency, the time period of oscillation of the total entropy production rate appears as half of the external frequency, but diffusion tends to destroy such symmetry over the two half cycles.

Appendix

6. Solution of probability for oscillating voltage case under diffusion

The solution of the above equation can be written as

$$\mathrm{P}_4(t) = P_4(t_0) \quad exp[-\int_{t_0}^{t} K_D(t^{'})dt^{'}] + \int_{t_0}^{t} \chi_D(t^{'}) \quad exp[-\int_{t}^{t} K_D(t^{''})dt^{''}]dt^{'}. \tag{36}$$

Using Eq.(36) one can write $\mathrm{P}_4(t)$ for $\mathrm{m}T < t < (m+1)T$ as[26]

$$\mathrm{P}_4(mT+t) = P_4(mT) \quad exp[-\int_{mT}^{t} K_D(t^{'})dt^{'}] + \int_{mT}^{t} \chi(t^{'}) \quad exp[-\int_{t}^{t} K_D(t^{''})dt^{''}]dt^{'}, \tag{37}$$

where T is the time period of the oscillating voltage and m ($= 0,1,2,....$) is the index of oscillation period. Now, using Eq.(36), one can write a recursion formula connecting the probabilities $\mathrm{P}_4(mT)$ and $\mathrm{P}_4((m+1)T)$ as

$$\mathrm{P}_4((m+1)T) = \phi P_4(mT) + \Delta_0, \tag{38}$$

where ϕ and Δ_0 are given by

$$\phi = exp\left[-\int_0^T K_D(t)dt\right] \tag{39}$$

and

$$\Delta_0 = \int_0^T \chi(t^{'}) \quad exp\left[-\int_{t}^{T} K_D(t^{''})dt^{''}\right]dt^{'}. \tag{40}$$

Above recursion relation gives the value of $\mathrm{P}_4(mT)$ as

$$\mathrm{P}_4(mT) = \phi^m P_4(0) + \frac{1-\phi^m}{1-\phi}\Delta_0, \tag{41}$$

where $\mathrm{P}_4(0)$ is the initial probability of the ion-conducting state. When $\mathrm{m} \to \infty$, the probability $\mathrm{P}_4(mT)$ approaches its asymptotic value,

$$\mathrm{lim}_{m\to\infty}\mathrm{P}_4(mT) = \frac{\Delta_0}{1-\phi}. \tag{42}$$

By substituting the above equation into Eq.(37) and taking the asymptotic long time limit of the probability, $\mathrm{P}_4(mT+t)$ which is denoted as $\mathrm{P}_4^{(ss)}(t)$, we obtain

$$\mathrm{P}_4^{(ss)}(t) = lim_{m\to\infty}\mathrm{P}_4(mT+t) = \frac{\Delta(t)}{1-\phi}. \tag{43}$$

Here the function $\Delta(t)$ is given by

$$\Delta(t) = \int_t^{t+T} \chi(t^{'}) \quad exp\left[-\int_{t^{'}}^{t+T} K_D(t^{''})dt^{''}\right]dt^{'}. \tag{44}$$

At very low frequency limit when $\mathrm{T} \to \infty$, ϕ defined in Eq.(39) vanishes. Therefore, $\mathrm{P}_4^{(ss)}(t)$ in Eq.(43) can be written as

$$\mathrm{P}_4^{(ss)}(t) = \int_0^T \chi_D(t-t^{'})exp[-\int_0^{t^{'}} K_D(t-t^{''})dt^{''}]dt^{'}. \tag{45}$$

As $\chi_D(t^{'})$ and $\mathrm{K}_D(t^{'})$ are slowly varying functions in the low frequency limit, we can take the following approximation

$$\chi_D(t-t^{'}) \approx \chi_D(t) - t^{'}\dot{\chi}_D(t^{'}), \mathrm{K}_D(t-t^{''}) \approx K_D(t) - t^{''}\dot{K}_D(t^{''})$$

and

$$\mathrm{exp}[-\int_0^{t^{'}} K_D(t-t^{''})dt^{''}] \approx \left(1+\frac{1}{2}\dot{K}_D(t)t^{'2}\right)exp[-K_D(t)t^{'}]. \tag{46}$$

Neglecting the term proportional to the product $\chi(t)K_D(t)$, we obtain

$$\mathrm{P}_4^{(ss)}(t) \approx Q(t) - \frac{\dot{Q}(t)}{K_D(t)}, \tag{47}$$

where $\mathrm{Q}(t) = \frac{\chi_D(t)}{K_D(t)}$. Then for slowly varying voltage, $\mathrm{P}_4^{(ss)}(t)$ finally becomes

$$\mathrm{P}_4^{(ss)}(t) = \frac{\chi_D(t)}{K_D(t)}. \tag{48}$$

Similarly, in the high frequency limit when $\mathrm{T} \to 0$, ϕ defined in Eq.(39) can be written as

$$\phi = 1 - T\langle K_D\rangle. \tag{49}$$

Here $\langle f\rangle = \frac{1}{T}\int_0^T f(t)dt$ where f can be $\chi_D(t)$ or $\mathrm{K}_D(t)$. Hence $\mathrm{P}_4^{(ss)}(t)$ in Eq.(43) takes the form

$$P_4^{(ss)}(t) = \frac{1}{T\langle K_D \rangle}\int_t^{t+T} \chi_D(t') \quad exp\left[-\int_{t'}^{t+T} K_D(t'')dt''\right]dt'. \tag{50}$$

In the high frequency limit we can take the following approximation

$$exp\left[-\int_{t'}^{t+T} K_D(t'')dt''\right] \approx 1-\int_{t'}^{t+T} K_D(t'')dt''. \tag{51}$$

Using this approximation, Eq.(50) can be written as

$$P_4^{(ss)}(t) = \frac{\int_t^{t+T}\chi_D(t')dt' - \int_t^{t+T}\chi_D(t')dt'\int_{t'}^{t+T}K_D(t'')dt''}{\int_t^{t+T}K_D(t')dt'}$$

$$= \frac{\langle \chi_D(t)\rangle}{\langle K_D(t)\rangle} - \delta(t). \tag{52}$$

Here we define $\delta(t) = \dfrac{\xi}{\int_t^{t+T}K_D(t')dt'}$ where $\xi = \int_t^{t+T}\chi_D(t')(\int_{t'}^{t+T}K_D(t'')dt'')dt'$. Here the limit t' varies in the range, $t \le t' \le t+T$ and t'' varies in the range, $t' \le t'' \le t+T$. In the double integration, ξ in the limit of $T \to 0$, one can approximate $(\int_{t'}^{t+T}K_D(t'')dt'')$ as $(T+t-t')K_D(t')$ where $0 \le (T+t-t') \le T$. This makes $\xi \approx T\int_t^{t+T}\chi_D(t')K_D(t')dt'$ and consequently $\delta(t) \to 0$ in the high frequency limit.

References

1. Nelson, D. L., Lehninger, A. L., & Cox, M. M. (2004). Lehninger principles of biochemistry. Macmillan. (4th ed., Worth Publishers, New York).
2. Shepherd, G. M. *Neurobiology*, (3rd ed., Oxford university press, New York, Oxford).
3. Hodgkin, A. L. (1952). AL Hodgkin and AF Huxley, J. Physiol. (London) 117, 500 (1952). *J. Physiol. (London), 117*, 500.
4. Sakmann, B., & Neher, E. (1995). *Single-Channel Recording* (2nd ed., Plenum Press, New York).
5. Hille, B. (2001). *Ion channels of excitable membranes* (Vol. 507). Sunderland, MA: Sinauer.
6. Yellen, G. (2002). The voltage-gated potassium channels and their relatives. *Nature*, *419*(6902), 35.
7. Long, S. B., Campbell, E. B., & MacKinnon, R. (2005). Crystal structure of a mammalian voltage-dependent Shaker family K+ channel. *Science*, *309*(5736), 897-903.
8. Jensen, M. Ø., Jogini, V., Borhani, D. W., Leffler, A. E., Dror, R. O., & Shaw, D. E. (2012). Mechanism of voltage gating in potassium channels. *Science*, *336*(6078), 229-233.
9. Kuang, Q., Purhonen, P., & Hebert, H. (2015). Structure of potassium channels. *Cellular and molecular life sciences*, *72*(19), 3677-3693.
10. Khalili-Araghi, F., Tajkhorshid, E., & Schulten, K. (2006). Dynamics of K+ ion conduction through Kv1. 2. *Biophysical journal*, *91*(6), L72-L74.
11. Khalili-Araghi, F., Tajkhorshid, E., Roux, B., & Schulten, K. (2012). Molecular dynamics investigation of the ω-current in the Kv1. 2 voltage sensor domains. *Biophysical journal*, *102*(2), 258-267.
12. Bezanilla, F. (2005). Voltage-gated ion channels. *IEEE transactions on nanobioscience*, *4*(1), 34-48.
13. Das, B., Banerjee, K., & Gangopadhyay, G. (2012). Entropy hysteresis and nonequilibrium thermodynamic efficiency of ion conduction in a voltage-gated potassium ion channel. *Physical Review E*, *86*(6), 061915.

14. Millonas, M. M., & Hanck, D. A. (1998). Nonequilibrium response spectroscopy and the molecular kinetics of proteins. *Physical review letters*, *80*(2), 401.
15. Millonas, M. M., & Hanck, D. A. (1998). Nonequilibrium response spectroscopy of voltage-sensitive ion channel gating. *Biophysical journal*, *74*(1), 210-229.
16. Kargol, A., Hosein-Sooklal, A., Constantin, L., & Przestalski, M. (2004). Application of oscillating potentials to the Shaker potassium channel. *General physiology and biophysics*, *23*, 53-76.
17. Kargol, A., Hosein-Sooklal, A., Constantin, L., & Przestalski, M. (2004). Application of oscillating potentials to the Shaker potassium channel. *General physiology and biophysics*, *23*, 53-76.
18. Keener, J. P. (2009). Invariant manifold reductions for Markovian ion channel dynamics. *Journal of Mathematical Biology*, *58*(3), 447-457.
19. Fox, R. F., & Lu, Y. N. (1994). Emergent collective behavior in large numbers of globally coupled independently stochastic ion channels. *Physical Review E*, *49*(4), 3421.
20. Collins, F. C. (1949). FC Collins and GE Kimball, J. Colloid Sci. 4, 425 (1949). *J. Colloid Sci.*, *4*, 425.
21. Gopich, I. V., Berezhkovskii, A. M., & Szabo, A. (2002). Concentration dependence of the diffusion controlled steady-state rate constant. *The Journal of chemical physics*, *117*(6), 2987-2988.
22. Berezhkovskii, A. M., & Szabo, A. (2013). Effect of ligand diffusion on occupancy fluctuations of cell-surface receptors. *The Journal of chemical physics*, *139*(12), 09B610_1.
23. Zagotta, W. N., Hoshi, T., & Aldrich, R. W. (1994). Shaker potassium channel gating. III: Evaluation of kinetic models for activation. *The Journal of general physiology*, *103*(2), 321-362.
24. Zagotta, W. N., Hoshi, T., Dittman, J., & Aldrich, R. W. (1994). Shaker potassium channel gating. II: Transitions in the activation pathway. *The Journal of general physiology*, *103*(2), 279-319.
25. Hoshi, T., Zagotta, W. N., & Aldrich, R. W. (1994). Shaker potassium channel gating. I: Transitions near the open state. *The Journal of General Physiology*, *103*(2), 249-278.
26. Pustovoit, M. A., Berezhkovskii, A. M., & Bezrukov, S. M. (2006). Analytical theory of hysteresis in ion channels: Two-state model. *The Journal of chemical physics*, *125*(19), 194907.